*Desalination and Water Treatment*
www.deswater.com

doi: 10.5004/dwt.2021.27885

243 (2021) 187–199
December

# Electrosorption of cadmium ions from the aqueous solution by a $MnO_2$/carbon fiber composite electrode

Jwan T. Hasan[a], Rasha H. Salman[b,*]

[a]*Department of Chemical Engineering, College of Engineering, University of Baghdad, Basrah, Iraq, Tel. +9647722091806; email: jwan.aljizani6@gmail.com*
[b]*Department of Chemical Engineering, College of Engineering, University of Baghdad, Al-Jadria, Baghdad, Post Code 10071, Iraq, Tel. +9647711959985; email: rasha.habeeb@coeng.uobaghdad.edu.iq/rashahabeb.rh@gmail.com, ORCID: 0000-0001-9353-9096*

Received 31 May 2021; Accepted 12 October 2021

---

## ABSTRACT

The nanostructured $MnO_2$/carbon fiber (CF) composite electrode was prepared using the anodic electrodeposition process. The crystal structure and morphology of $MnO_2$ particles were determined with X-ray diffraction and field-emission scanning electron microscopy. The electrosorptive properties of the prepared electrode were investigated in the removal of cadmium ions from aqueous solution, and the effect of pH, cell voltage, and ionic strength was optimized and modeled using the response surface methodology combined with Box–Behnken design. The results confirm that the optimum conditions to remove Cd(II) ions were: pH of 6.03, a voltage of 2.77 V, and NaCl concentration of 3 g/L. The experimental results showed a good fit for the Freundlich isotherm model and the pseudo-second-order kinetic model.

*Keywords:* Cadmium ions; Carbon fiber; Electrodeposition; Electrosorption; Nanostructured manganese dioxide

---

## 1. Introduction

The continuous use of water in various activities, whether domestic, industrial, or agricultural, produces wastewater effluents containing different types of harmful and unwanted pollutants [1–3]. Heavy metals are considered the most serious types of pollutants that threaten the aquatic environment with its living and non-living components. Such metals pose significant risks to human health and aquatic ecosystems due to their non-biodegradability thus tend to be absorbed and accumulated in living organisms over time [4–6]. Cadmium is one of the most hazardous heavy metals found in wastewater which is often released from electroplating, pigment manufacture, electronic compounds, polymerization process, and plastic production [7,8]. Cadmium is classified as a probable human carcinogen and chronic exposure to it results in many health problems [3]. There are several treatment techniques that have been used to remove cadmium ions from wastewater, such as ion exchange, adsorption, and chemical precipitation, however, these techniques are usually limited thus far due to technical or economic limitations, particularly at low cadmium concentrations [9,10]. Compared to these treatment techniques, the electrosorption process, or referred to as capacitive deionization technology (CDI), is a new and promising technology for removing ionic species from aqueous solutions [11,12]. The electrosorption process has many advantages such as low energy consumption, simple operation, easy regeneration, environmentally friendly, and has no secondary pollution [13–15]. The working principle of the electrosorption process is based on applying an external electric field between the electrodes making the ionic species in the aqueous solution move towards the oppositely charged electrode to be absorbed onto the electrode surface and when the electric current is removed or reversed, the ions are released back into the solution [16,17]. The electrode material and its physical properties are considered to

---

* Corresponding author.

1944-3994/1944-3986

be the most important factor in the electrosorption process. The electrodes used are preferable of a high surface area, good electrical conductivity, high specific capacitance, stable electrochemical performance [9,18]. Conventional capacitive deionization CDI uses the carbonaceous materials as electrodes such as carbon fiber [19], carbon nanotube [20], carbon aerogel [21], glassy carbon [22], etc. which are characterized by a high surface area, high conductivity, long cycling lives [23]. During the charging step, an electrical double layer (EDL) is formed at the carbon surface/solution interface and the ions are absorbed onto the carbon surface until reach its maximum ions adsorption capacity [24]. Due to the EDLs nature of the carbonaceous materials, their specific capacitances, interaction with metal ions, and selectivity are somewhat low [25]. To enhance the performance of the carbonaceous electrodes in the electrosorption process for ions removal, the composite electrode can be produced using the pseudocapacitive materials based on Faradaic ion storage where reversible redox reactions can be occurred to provide the electrode capacitance [24]. The most widely pseudocapacitive materials used are the transition metal oxides (TMOs) such as titanium dioxide ($TiO_2$), manganese dioxide ($MnO_2$), ruthenium dioxide ($RuO_2$), nickel oxide (NiO), etc. [22,23]. Among these transition metal oxide, manganese dioxide ($MnO_2$) is one of the most attractive pseudocapacitive materials and effective adsorbents due to the unique structures, high specific capacitance (close to 1370 F/g), natural abundance, good cycle stability, low toxicity, eco-friendly, and low cost [25–27]. $MnO_2$ can be fabricated with different morphologies and has many valence states as well as crystal structures such as α-, β-, γ-, and δ-$MnO_2$ [27]; γ- and α- phases give a higher surface area than the other phases [25]. $MnO_2$/carbon composite electrode shows a significantly improved adsorption ability lead to better performance for the electrosorption process of ions [19].

In the present work, the $MnO_2$/carbon fiber composite electrode was manufactured using the electrodeposition process and the structure and morphology of the $MnO_2$ particles were examined. The performance of the prepared electrode in electrosorption of the cadmium ions from an aqueous solution was tested under different combinations of pH value, cell voltage, and ionic strength (NaCl concentration). These selected operating parameters and their interactive effects on the cadmium ions removal efficiency were optimized and studied adopting the response surface methodology using Box–Behnken experimental design.

## 2. Experimental work

### 2.1. Materials

All chemicals utilized in the experiments were of analytical grade and there was no need for purification. The electrolytic solution in the part of the preparation of the electrochemical electrode consisted of manganese(II) sulfate monohydrate ($MnSO_4{\cdot}H_2O$) (98%, HiMedia, India), and sulfuric acid ($H_2SO_4$) (98%, Central Drug House (P) Ltd., India). While in the experiments of cadmium ions removal, cadmium sulfate (1:1) hydrate (3:8) ($3CdSO_4{\cdot}8H_2O$) (99%, BDH Chemicals Ltd., UK) and sodium chloride (NaCl) (99.9%, Central Drug House (P) Ltd.) were used.

### 2.2. Preparation of electrodes

To prepare the $MnO_2$/carbon fiber composite electrode, a facile method as the anodic electrodeposition process was used. As a preliminary work, the commercial carbon fiber that was utilized as a substrate was firstly cut into rectangle straps (12 cm × 5 cm). Then these straps were activated and treated for 30 min with 5% $HNO_3$ (69%, Hopkin & Williams Ltd., UK) at 80°C and then rinsed with distilled water. The electrodeposition process of $MnO_2$ onto the carbon fiber was conducted galvanostatically at a current density of (0.5 mA/cm$^2$) using a regulated DC power supply (UNI-T: UTP3315TF-L) for 4 h. The electrochemical solution was prepared by mixing 2 L of distilled water with 0.34 M $H_2SO_4$ and 0.35 M $MnSO_4$. A hot plate magnetic stirrer (LABINCO L81) was utilized to mix the electrolytic solution well and raise its temperature to 90°C. The fabric substrate was soaked in the electrolyte for 2 h at 90°C before starting the electrodeposition process. The electrochemical cell consisted of two electrodes: the anode material was the pre-treated carbon fiber strap, and the counter cathode was a pair of graphite pieces, and both of which were fixed inside the glass electrolytic bath. After electrodeposition, the $MnO_2$/carbon fiber electrode was washed with distilled water several times and then dried. The prepared electrode was kept for later use in the electrosorption process.

### 2.3. Structural characterization

The crystallographic characteristics of the deposited manganese oxide ($MnO_2$) films were examined by X-ray diffraction (XRD, Philips X'PERT, Holland) using Cu-Kα radiation as the X-ray source with ($\lambda = 1.54056$°A). The diffraction data were collected over 2θ, ranging from 0° to 90°. Field-emission scanning electron microscopy (FESEM, TESCAN Mira3, France) was used to characterize the surface morphologies of the electrochemically deposited electrode equipped with an electron energy-dispersive X-ray spectrometry (EDX) analyzer to examine the surface composition.

### 2.4. Electrosorption experiment

To investigate the electrosorptive properties of the prepared electrode ($MnO_2$/carbon fiber) for cadmium ions removal, a small lab-scale experimental electrosorption apparatus as illustrated in the photo and the schematic diagram was used as shown in Fig. 1.

The electrolytic cell was a 1 L glass beaker that contained an aqueous solution with 100 mg/L as a constant initial cadmium ions concentration and $x$ of NaCl concentration in g/L. The electrodes were immersed in the aqueous solution. One strap of the prepared electrode ($MnO_2$/carbon fiber) was used as a cathodic substrate (working electrodes), while two straps of pure carbon fiber were utilized as anodes (Counter electrodes). The cathode was placed between the two anodes at a distance of 2 cm from each other. A regulated DC power supply (BAKU: BK-305D) was used with a hot plate magnetic stirrer (LABINCO L81) to continuously stir the aqueous solution during the experiment to ensure ionic diffusion. The experiments were performed at room temperature under different operating parameters:

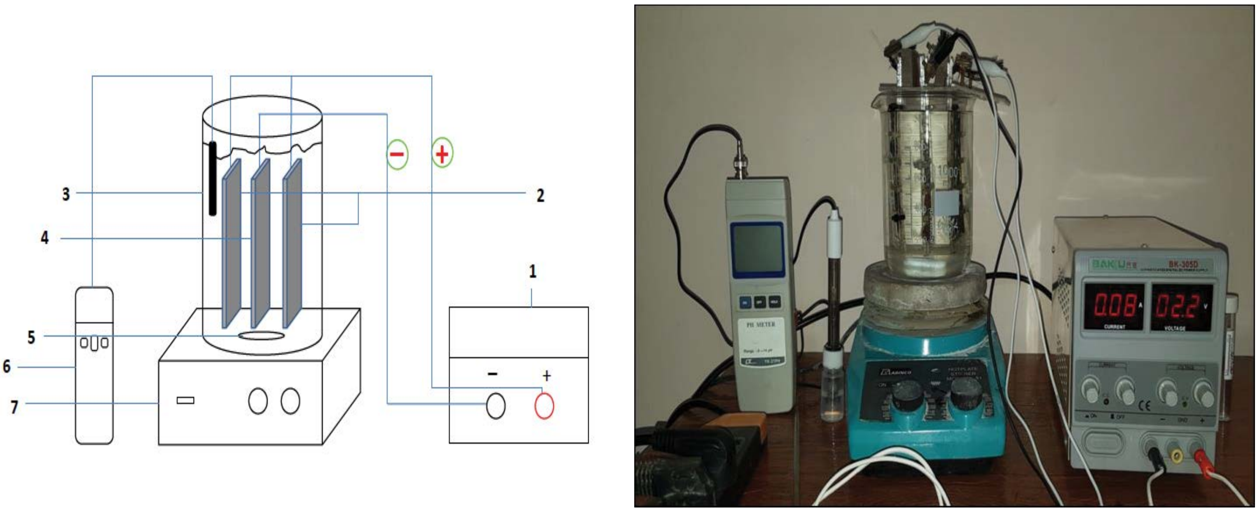

Fig. 1. Photo and schematic diagram of the electrosorption system; 1. Regulated DC power supply, 2. Pair of pure carbon fiber straps (anode), 3. Beaker, 4. $MnO_2$/carbon fiber (cathode), 5. Magnetic bar, 6. pH meter, 7. Hot plate magnetic stirrer.

pH (3–8), cell voltage (2.2–3 V), NaCl concentration (1–3 g/L). The concentration of cadmium ions in the solution was analyzed by flame atomic absorption spectrometry (AAS) (AAS SensAA GBC). The pH of the solution was measured using a pH meter (Lutron: YK-21PH, United States) and adjusted by adding 0.1 M sodium hydroxide (97%, Sigma-Aldrich, United States) or 0.1 M hydrochloric acid (37%, Thomas Baker, India). The removal efficiency and the equilibrium adsorption capacity $q_e$ (mg/g) were calculated as follows [10]:

$$\text{Re}(\%) = \frac{(C_0 - C_e)}{C_0} \times 100 \tag{1}$$

$$q_e = \frac{(C_0 - C_e)}{m} V \tag{2}$$

where $C_0$ (mg/L) and $C_e$ (mg/L) are the initial and equilibrium concentrations of cadmium ions in the solution, $m$ is the total mass of the electrode and $V$ is the solution volume.

### 2.5. Design of experiments

Response surface methodology (RSM) is a combination of various statistical and mathematical approaches that are useful for designing, developing, and optimizing processes. This method can be used for assessing the effects of different individual parameters, their relative significance, the interaction among the parameters, and determining the optimal conditions for the required responses. RSM has important applications in many processes in the chemical engineering and applied sciences to optimize and evaluate the interactive effects of their operating parameters, like the capacitive deionization process (electrosorption) [8,28–30].

In the present study, the optimum conditions for the electrosorption of cadmium ions were determined utilizing Box–Behnken (BBD) experimental design.

The advantage of the BBD is that it permits using relatively few parameter combinations to determine the complex response function [31]. A 3-level, 3-factor BBD was employed to investigate the effect of the selected parameters on the removal efficiency of Cd(II) ions from aqueous solution using the $MnO_2$/carbon fiber electrode. The three operating parameters of pH value ($X_1$), cell voltage ($X_2$), and NaCl concentration ($X_3$) were chosen as process variables, while the removal efficiency ($Y$) of Cd(II) ions was considered as the response. The design is composed of three levels: low, medium, and high coded as −1, 0, and +1. The parameters were coded according to the following equation:

$$x_i = \frac{X_i - X_0}{\Delta X_i} \tag{3}$$

where $x_i$ is the coded value of a parameter, $X_i$ is the real value of a parameter, $X_0$ is the real value of a parameter at the center point and $\Delta X_i$ is the step change value [32]. Process parameters with their coded levels are shown in Table 1. A polynomial model of second-order or also called quadratic model can be used for further modeling of experimental results, where interaction terms equipped with the experimental data obtained from the Box–Behnken model experiment, according to the following equation:

$$Y = a_0 + \sum a_i x_i + \sum a_{ii} x_i^2 + \sum a_{ij} x_i x_j \tag{4}$$

where ($Y$) is the removal efficiency of cadmium ions (response), $x_i$, $x_j$, … , $x_k$ are the input parameters of the process, $a_0$ is the intercept term, $a_i$ is the linear effect, $a_{ii}$ is the squared effect, and $a_{ij}$ is the interaction effect. In this study, a total of 15 experiment combinations are needed to calculate 10 coefficients of the second-order polynomial equation [31]. A set of 15 experimental runs, which were designed using BBD for cadmium ions removal, including duplicates, is shown in Table 1.

The data were analyzed for variance and the regression coefficient ($R^2$) was calculated to determine the goodness of fit of the model.

## 3. Results and discussion

### 3.1. Morphological and structural characterization

The XRD analysis was used for demonstrating the presence of $MnO_2$ particles on the carbon fiber surface and examining their crystal structures. Fig. 2 shows the XRD pattern of the deposited $MnO_2$. This pattern demonstrated the crystalline structure of $MnO_2$ particles on the carbon fiber surface. It should be noted that the sharp and intense diffraction peaks show the good crystallization of the product [33]. The diffraction peaks at around 26° and 43.5° are associated with carbon fiber. Other peaks that appeared are associated with $MnO_2$ diffraction peaks, which can be indexed as γ-$MnO_2$ phase as in [27,34,35]. The XRD peaks of $MnO_2$ that recorded at 2θ are 37.27°, 42.69°, 44.209°, 56.22°, and 64.62°.

Table 1
Box–Behnken experimental design for cadmium ions removal

| Run | Blk | Coded value | | | Real value | | |
|---|---|---|---|---|---|---|---|
| | | $X_1$ | $X_2$ | $X_3$ | pH | Voltage (V) | NaCl concentration (g/L) |
| 1 | 1 | +1 | –1 | 0 | 8 | 2.2 | 2 |
| 2 | 1 | +1 | 0 | –1 | 8 | 2.6 | 1 |
| 3 | 1 | –1 | 0 | +1 | 3 | 2.6 | 3 |
| 4 | 1 | 0 | +1 | +1 | 5.5 | 3 | 3 |
| 5 | 1 | 0 | –1 | –1 | 5.5 | 2.2 | 1 |
| 6 | 1 | 0 | –1 | +1 | 5.5 | 2.2 | 3 |
| 7 | 1 | –1 | –1 | 0 | 3 | 2.2 | 2 |
| 8 | 1 | 0 | 0 | 0 | 5.5 | 2.6 | 2 |
| 9 | 1 | +1 | 0 | +1 | 8 | 2.6 | 3 |
| 10 | 1 | 0 | +1 | –1 | 5.5 | 3 | 1 |
| 11 | 1 | –1 | +1 | 0 | 3 | 3 | 2 |
| 12 | 1 | 0 | 0 | 0 | 5.5 | 2.6 | 2 |
| 13 | 1 | +1 | +1 | 0 | 8 | 3 | 2 |
| 14 | 1 | –1 | 0 | –1 | 3 | 2.6 | 1 |
| 15 | 1 | 0 | 0 | 0 | 5.5 | 2.6 | 2 |

The morphology of as-deposited $MnO_2$ particles onto the CF surface imaged by FESEM is shown in Fig. 3. Fig. 3a represents a FESEM micrograph of the carbon fibers before the $MnO_2$ deposition process, which appears with a smooth surface. The results refer (Fig. 3b) that the $MnO_2$ particles deposited on the carbon fibers surface was with flower-like nanostructure as in [36], and these flower-like nanostructures, at high magnifications (Fig. 3c), appear to consist of many $MnO_2$ nanorods and this has been noted as well by [37]. The average diameters of the electrodeposited $MnO_2$ nanoparticles were 73.38 nm. As it is evident, most of the carbon fiber surface was covered by the $MnO_2$ particles and these particles tended to merge to create a thin film with a uniform structure and high capacitance in the ion charge process due to the large surface area [38,39].

The EDX result of the composite electrode is depicted in Fig. 4. The result confirms that the main chemical elements present on the surface of the carbon fibers are Mn and O, with very small amounts of S and Si. Fig. 4a represents the EDX analysis of the pure carbon fibers containing 0% Mn on their surface.

### 3.2. Response surface model analysis for electrosorption process

#### 3.2.1. Model fitting and statistical analysis

The BBD model was utilized to design the experiments statistically to optimize and study the interactive effects of the selected operating parameters of the electrosorption

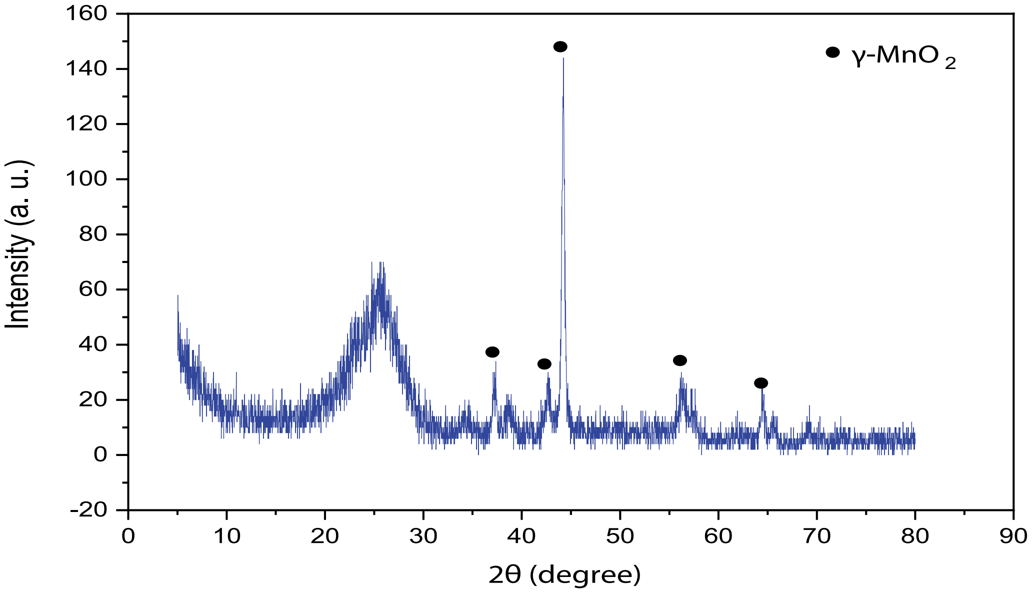

Fig. 2. XRD analysis of $MnO_2$ film on CF substrate at C.D. of 0.5 mA/cm$^2$, 0.35 M $MnSO_4$ and 4 h.

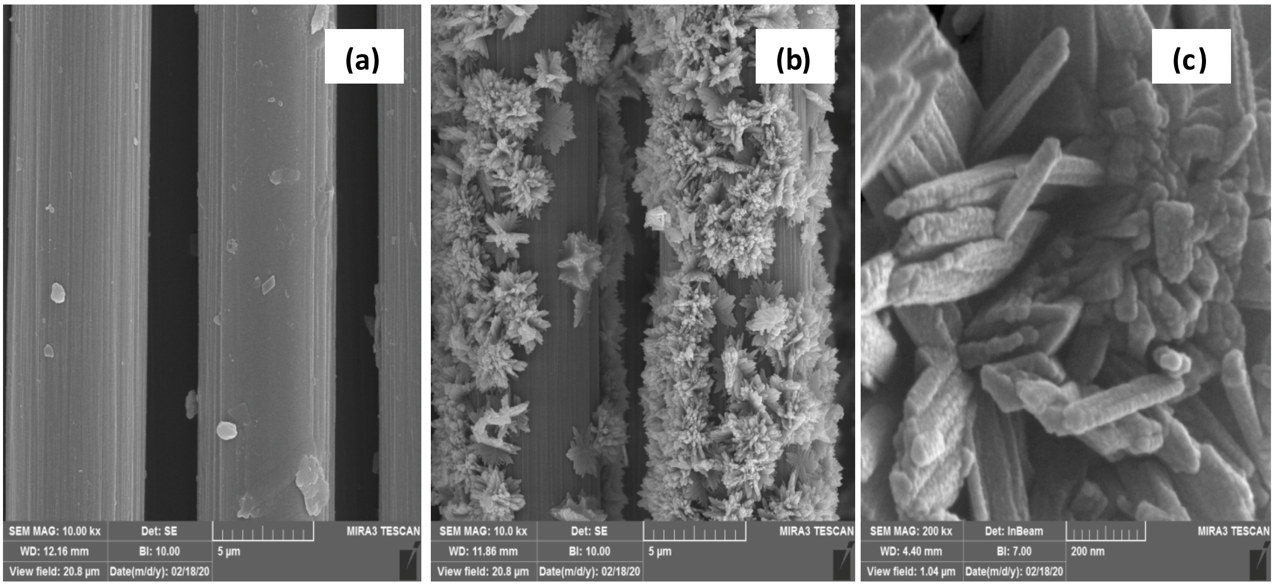

Fig. 3. FESEM micrographs of $MnO_2$ film on CF substrate (a) pure CF and (b,c) CF coated with $MnO_2$ at C.D. of 0.5 mA/cm², 0.35 M $MnSO_4$, and 4 h.

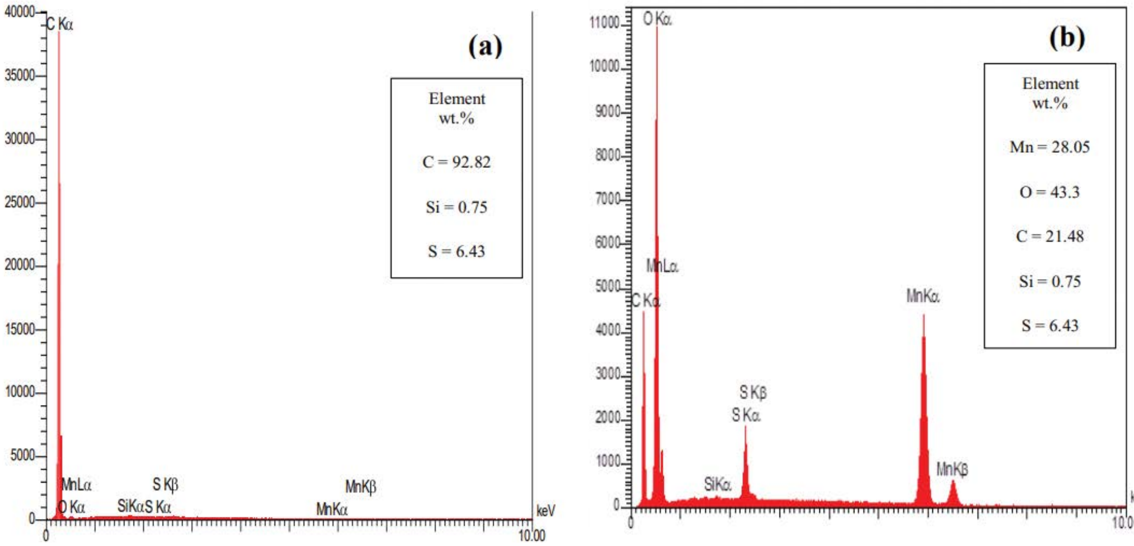

Fig. 4. EDX results of $MnO_2$ film on CF substrate (a) pure CF and (b) CF coated with $MnO_2$ at C.D. of 0.5 mA/cm², 0.35 M $MnSO_4$, and 4 h.

process on the cadmium ions removal efficiency using the $MnO_2$/carbon fiber composite electrode.

Fifteen experimental runs have been conducted under different combinations of pH, cell voltage, and NaCl concentration to identify which parameters and their interactions have a significant impact on the removal efficiency of cadmium ions. Table 2 illustrates the measured values of the process response represented by the removal efficiency of Cd(II) ions. Minitab-17 software was used for experimental data analysis.

By using the method of least squares (MLS) which is a multiple regression analysis techniques, the experimental data were fitted into a polynomial–quadratic model to get the regression equation. The final empirical regression equation which represents the relationship between the cadmium ions removal efficiency and the three operating parameters in terms of coded units is given in Eq. (5) as the software suggested.

$$\begin{aligned} Y_{Cd^{+2}} = & -215.3 - 1.75X_1 + 221.4X_2 + 9.25X_3 \\ & - 0.202X_1X_1 - 39.10X_2X_2 - 0.375X_3X_3 \\ & + 0.896X_1X_2 + 0.568X_1X_3 - 3.37X_2X_3 \end{aligned} \quad (5)$$

where $Y$ is the removal efficiency for cadmium ions, namely, the response; $X_1$, $X_2$, and $X_3$ are the values of the operating parameters, pH ($X_1$), cell voltage ($X_2$), NaCl concentration ($X_3$). The positive coefficients in the equations demonstrate the compatible effects on the response, whereas the negative coefficients show their incompatible effects.

To evaluate the statistical significance and the appropriateness of the suggested quadratic models, the analysis of variance (ANOVA) was applied. ANOVA is a statistical method used to test the suppositions on the model coefficients by subdividing the total variance in a set of experimental data; associated with a specific process, into defined parts related to sources of variation [40]. The ANOVA analysis was determined based on the degree of freedom (DOF), sum of square (SS), percentage contribution %, mean of square (MS), adjusted mean of square (Adj. MS), adjusted sum of squares (Adj. SS), *F*-value, and *P*-value. The ANOVA results are given in Table 3.

Table 2
Experimental results of BBD for cadmium ions removal

| Run | Blk | pH | Voltage (V) | NaCl concentration (g/L) | Re% | |
|---|---|---|---|---|---|---|
| | | | | | Act. | Pred. |
| 1 | 1 | 8 | 2.2 | 2 | 81.97 | 82.88 |
| 2 | 1 | 8 | 2.6 | 1 | 92.57 | 92.39 |
| 3 | 1 | 3 | 2.6 | 3 | 99.25 | 99.43 |
| 4 | 1 | 5.5 | 3 | 3 | 98.91 | 99.64 |
| 5 | 1 | 5.5 | 2.2 | 1 | 83.07 | 82.21 |
| 6 | 1 | 5.5 | 2.2 | 3 | 91.64 | 90.03 |
| 7 | 1 | 3 | 2.2 | 2 | 85.78 | 87.21 |
| 8 | 1 | 5.5 | 2.6 | 2 | 98.57 | 98.97 |
| 9 | 1 | 8 | 2.6 | 3 | 99.02 | 99.73 |
| 10 | 1 | 5.5 | 3 | 1 | 96.73 | 98.34 |
| 11 | 1 | 3 | 3 | 2 | 99.14 | 98.23 |
| 12 | 1 | 5.5 | 2.6 | 2 | 99.29 | 98.97 |
| 13 | 1 | 8 | 3 | 2 | 98.91 | 97.48 |
| 14 | 1 | 3 | 2.6 | 1 | 98.48 | 97.78 |
| 15 | 1 | 5.5 | 2.6 | 2 | 99.03 | 98.97 |

In the ANOVA results tables, the percentage contribution for each coefficient is defined as a portion of the total variance that occurred in the experiment for each significant coefficient, so the higher the percentage contribution of a specific coefficient, the more it contributes to the final results than the other coefficients, and any small variation in its value will have a great effect on the response [41].

As shown in the ANOVA results, the cell voltage has a high contribution percentage of 60.28% compared to the contribution percentages of the pH value and the NaCl concentration which have a low effect on the response. The linear term has the main contribution percentages with 68.93%, while the square term and 2-way interaction term contribute by 25.96% and 3.28%, respectively. The significance of each coefficient in the model on the response was determined by the *F*-values and *P*-values, where high significance was represented by higher *F*-values and lower *P*-values [8]. The *F*-value is the ratio of the mean square of the model (MS) to the appropriate error mean square. The greater the ratio, the greater the *F*-value, and the greater the probability that the model's variance is significantly greater than random error [29]. The Probability value (*P*-value) is used to determine statistically significant effects in the model. *P*-value less than 0.05 indicates that the effect of the coefficients is statistically significant at a 95% confidence level [42]. The ANOVA results revealed that the *F*-value of 29.77 for Cd(II) ions removal is greater

Table 3
Analysis of variance for cadmium removal

| Source | DOF | Seq. SS | Contr. (%) | Adj. SS | Adj. MS | *F*-value | *P*-value |
|---|---|---|---|---|---|---|---|
| Model | 9 | 555.310 | 98.17 | 555.310 | 61.701 | 29.77 | 0.001 |
| Linear | 3 | 389.943 | 68.93 | 389.943 | 129.981 | 62.70 | 0.000 |
| $X_1$ | 1 | 12.936 | 2.29 | 12.936 | 12.936 | 6.24 | 0.055 |
| $X_2$ | 1 | 340.984 | 60.28 | 340.984 | 340.984 | 164.49 | 0.000 |
| $X_3$ | 1 | 36.023 | 6.37 | 36.023 | 36.023 | 17.38 | 0.009 |
| Square | 3 | 146.834 | 25.96 | 146.834 | 48.945 | 23.61 | 0.002 |
| $X_1X_1$ | 1 | 2.317 | 0.41 | 5.874 | 5.874 | 2.83 | 0.153 |
| $X_2X_2$ | 1 | 143.999 | 25.46 | 144.475 | 144.475 | 69.70 | 0.000 |
| $X_3X_3$ | 1 | 0.518 | 0.09 | 0.518 | 0.518 | 0.25 | 0.638 |
| 2-way interaction | 3 | 18.533 | 3.28 | 18.533 | 6.178 | 2.98 | 0.135 |
| $X_1X_2$ | 1 | 3.209 | 0.57 | 3.209 | 3.209 | 1.55 | 0.269 |
| $X_1X_3$ | 1 | 8.071 | 1.43 | 8.071 | 8.071 | 3.89 | 0.105 |
| $X_2X_3$ | 1 | 7.252 | 1.28 | 7.252 | 7.252 | 3.50 | 0.120 |
| Error | 5 | 10.365 | 1.83 | 10.365 | 2.073 | – | – |
| Lack-of-fit | 3 | 10.094 | 1.78 | 10.094 | 3.365 | 24.84 | 0.039 |
| Pure error | 2 | 0.271 | 0.05 | 0.271 | 0.135 | – | – |
| Total | 14 | 565.674 | 100.00 | – | – | – | – |
| Model summary | | S. | $R^2$ | $R^2$ (Adj.) | PRESS | $R^2$ (Pred.) | |
| | | 1.43977 | 98.17% | 94.87% | 162.109 | 71.34% | |

than the critical *F*-value for the significance level of 0.05 with freedom degrees equal to 9, which means that the model is statistically significant. The *P*-value of 0.001 ($<0.05$) implies that the model has a highly significance and could be utilized for the prediction of the results of the electrosorption process. Therefore, it is observed; by analyzing the *F*-value and *P*-value, the $X_2$ and $X_2 \cdot X_2$ terms are the most significant terms in the model.

The multiple correlation coefficient ($R^2$) is used to evaluate the goodness of the fitting model. It is observed from Table 3 that the value of $R^2$ is 0.9817, which showed that this regression was statistically significant and the model did not explain only 1.83% of the total variance.

### 3.2.2. Main effect plot

The main effect plot can display the relationship between the response and the selected operating parameters. Fig. 5 represents the main effect plot that illustrates the effects of the pH solution, cell voltage, and ionic strength on the cadmium ions removal efficiency by applying the electrosorption process. It is evident from the figure that the cell voltage has the main influence on the removal efficiency as also observed in the ANOVA analysis and the model regression equation.

In the electrosorption process, the removal efficiency of cations increases with increasing the value of solution pH. This is attributed to the fact that the surface potential of the electrode becomes more negative when the pH value increases, which leads to an increase in the electrostatic attraction between the positive ions and the electrode surface. While the electrostatic repulsion increases at a low pH value. In addition, at a high solution pH, the concentration of the $H_3O^+$ becomes lower and thus becomes less competitive with the positive ions for the adsorption sites [18,19]. As shown in the main effect plot, the removal efficiency of cadmium ions increases with increasing the value of solution pH but then slightly decreases as the pH was further increased.

By applying a higher voltage between the electrodes, the electron flow velocity is accelerated and the electrostatic attraction between the ions and electrode surface becomes stronger [19], resulting in larger amounts of ions electrosorbed onto the electrode surface. Therefore, the electrosorption of the cadmium ions was enhanced and the removal efficiency increased with increasing the applied voltage. This is also observed in the main effect plot.

Both natural water and wastewater usually contain different ions, which can affect and interfere with the absorption of the other ions [9]. To study the effect of ionic strength on cadmium ions adsorption, NaCl was used as a supporting electrolyte. It is observed from the main effect plot, that the removal efficiency increases as the NaCl concentration increases from 1 to 3 g/L. Increasing NaCl concentration can improve the conductivity of the solution that leads to enhance the removal efficiency. When large amounts of NaCl are added, the removal efficiency may begin to decrease due to the competitive adsorption between the Na(I) and Cd(II) ions as observed in [9].

To visualize the predicted model equation and illustrate the variation that occurs when two or more parameters change together, the response surface plot and contour plot can be utilized. The response surface plot is a three-dimensional plot that displays the relationship between the response and the independent parameters. The two-dimensional plot corresponding to the surface plot is called the contour plot which helps in visualizing the shape of the response by drawing the lines of the constant response in the plane of the independent parameters [43].

The response surface and contour plots that showing the interactive effects of the selected operating parameters on the removal efficiency of cadmium ions are depicted in Fig. 6. The combined effects on the removal efficiencies were tested by varying $X_1$ (pH) from 3 to 8, $X_2$ (cell voltage)

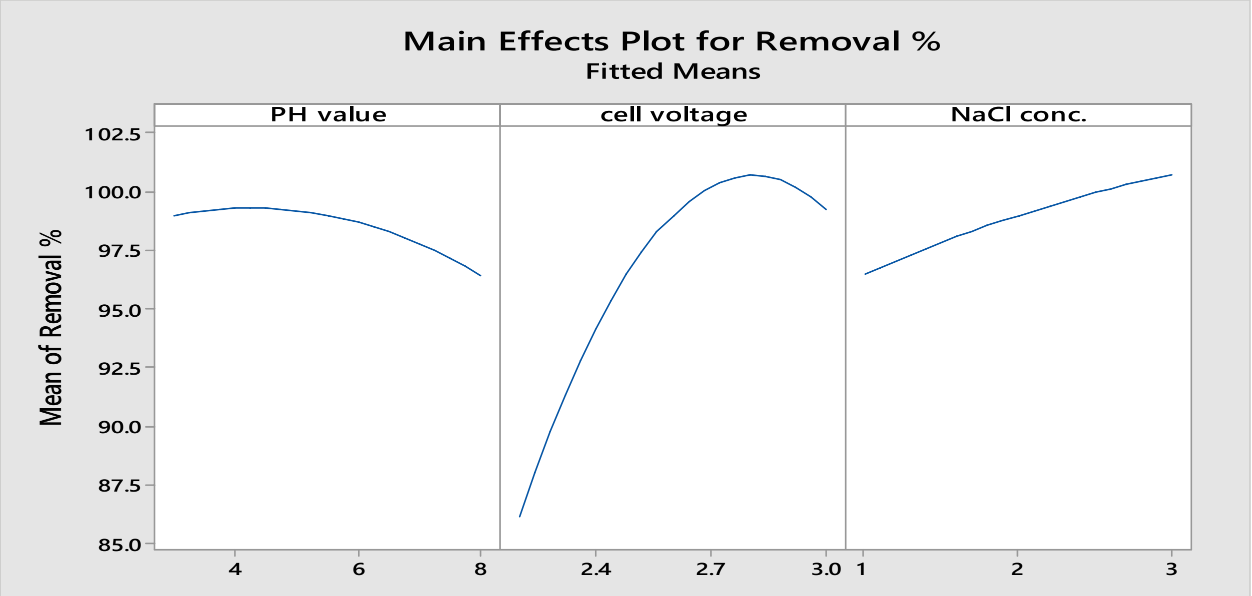

Fig. 5. Main effect plot for cadmium ions removal.

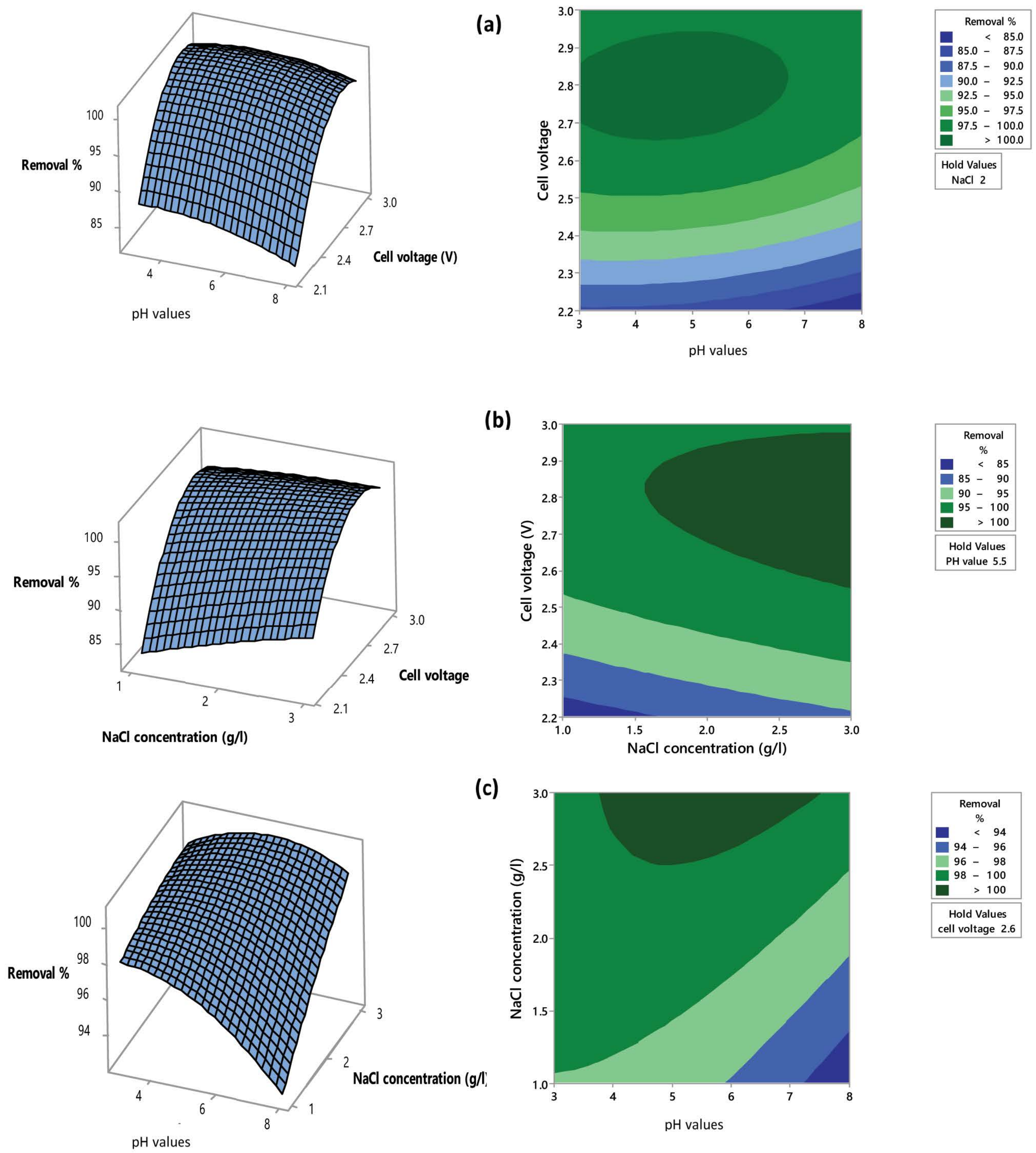

Fig. 6. Response surface and contour plots for the effect of (a) solution pH and cell voltage (V), (b) NaCl concentration (g/L) and cell voltage (V), and (c) solution pH and NaCl concentration (g/L) on the cadmium removal (%).

from 2.2 to 3 V, and $X_3$ (NaCl concentration) from 1 to 3 g/L for cadmium ions removal.

As observed in the surface plot in Fig. 6a, there is a slight decrease in the removal efficiency with increasing the pH value at a voltage of 2.2 V, whereas no significant effect of pH at 3 V. On the other hand, with pH 3 the removal efficiency increased with increasing the voltage up to 2.9 V and then declined slightly as well as for pH 8. The corresponding contour plot displays an ellipse area representing the maximum values of the removal efficiency where the pH value are ranging from 3 to 6.7 and the voltage ranging from 2.7 to 2.85 V.

Fig. 6b explains that at any value of NaCl concentration (1–3 g/L), the removal efficiency increased with increasing the applied voltage and then slightly declined as it approaches 3V. At the voltage of 2.2, there is no significant effect in the removal efficiency with increasing the NaCl concentration, whereas there is a slight increase at the voltage of 3 V. It is obvious from the contour plot that the area of maximum values of the removal efficiency is confined between the NaCl concentration values (1.7–3 g/L) and the voltages (2.55–2.98 V).

Fig. 6c shows that at pH 8, the removal efficiency of cadmium ions increased steeply linearly with increasing the NaCl concentration from 1 to 3 g/L, whereas there is no significant effect of NaCl concentration at pH 3. On the other hand, at 1 g/L of NaCl concentration, the removal efficiency decreased with increasing the pH value, while at 3 g/L NaCl concentration, the removal efficiency increased with increasing the pH value up to 7.5 and then declined slightly. The corresponding contour plot confirms the maximum values of the removal efficiency lie in the pH value range 3.7–7.5 and the NaCl concentration range of 2.4–3 g/L.

### 3.3. Optimization and confirmation test

Optimizing the operating parameters for any electrochemical removal system is essential for determining the conditions at which the highest removal efficiency and lower energy consumption can be obtained. The optimization was attained by applying the RSM regression equation with the desirability function technique ($D_F$). Depending on this function, the quality characteristics of each predicted response are represented by a dimensionless desirability value that ranges from 0 to 1, and as this value increases, the desirability of the response increases [44].

When optimizing the electrosorption process of cadmium ions from aqueous solution and regarding goal fields, the selected operating parameters of pH ($X_1$), cell voltage ($X_2$), NaCl concentration ($X_3$) were within the range and the results, namely, removal efficiency ($Y$) was maximized with a corresponding weight of 1.0. For cadmium ions removal, the ranges of the parameters: pH (3–8), cell voltage (2.2–3 V), and NaCl concentration (1–3 g/L). The limit values of the removal efficiency were specified with the lower value of 81.97% and the upper value of 99.29%. Under these limits and conditions, the optimizing for the cadmium removal process was carried out and the results are depicted in Table 4, with a desirability function of (1) for the model.

To confirm the adequacy of the developed model, repeated experiments can be conducted under the optimal conditions and the results of these experiments are expected to be within the specified range obtained from the optimization analysis. The result of the confirmation experiments is shown in Table 5. Two experiments at the optimized operating parameters were performed. The removal efficiency was 99.542% and the value was within the range of the optimal value expected.

### 3.4. Adsorption isotherms

A preliminary experiment for the electrochemical adsorption processes of cadmium ions from an aqueous solution was performed to determine the equilibrium time required for the $MnO_2$/carbon fiber composite electrode to reach its saturated adsorption point. The preliminary experiment was carried out at pH 5.5, 2.6 V, and 2 g/L NaCl concentration. The results showed that the best period time for reaching the equilibrium at Cd(II) ions removal process, was approximately 300 min (5 h). Fig. 7 illustrates the curve of the adsorption capacity ($q_t$) vs. the contact time ($t$) between the electrode surface and the solution.

Adsorption isotherms can be defined as suitable mathematical models to describe the distribution of the adsorbed ions between the adsorbent material and the solution at equilibrium. The adsorption data were analyzed by utilizing the Langmuir and Freundlich isotherm models that relate the amount of adsorbed ions $q_e$ (mg/g) to the equilibrium

Table 4
Optimal performance of system variables for the maximum removal of cadmium

| Response | Goal | | Lower | Target | Upper | Weight | Importance |
|---|---|---|---|---|---|---|---|
| Re (%) | Maximum | | 81.97% | Maximum | 99.29% | 1 | 1 |
| | Solution: parameters | | Results | | | | |
| pH | Cell voltage (V) | NaCl conc.(g/L) | Re (%) fit | $D_F$ | SE fit | 95 % CI | 95 % PI |
| 6.03 | 2.77 | 3 | 101.841 | 1 | 0.942 | (99.42, 104.263) | (97.419, 106.264) |

Table 5
Confirmation experiments of cadmium ions removal

| Run | pH | Cell voltage (V) | NaCl conc. (g/L) | Re (%) | | AC (mg/g) |
|---|---|---|---|---|---|---|
| | | | | Actual | Average | |
| 1 | 6.03 | 2.77 | 3 | 99.334% | 99.542% | 41.91 |
| 2 | 6.03 | 2.77 | 3 | 99.75% | | 42.09 |

concentration $C_e$ (mg/g) [45]. Langmuir and Freundlich isotherm models represented by linearized equations as follows [46], respectively:

$$q_e = \frac{q_m b C_e}{1 + bC_e} \quad (6)$$

$$q_e = K_F C_e^{1/n} \quad (7)$$

where $q_e$ (mg/g) is the equilibrium adsorption capacity, $C_e$ (mg/L) is the equilibrium concentration, $q_m$ (mg/g) is the maximum adsorption capacity of the adsorbent, $b$ is the Langmuir constant of equilibrium adsorption, $K_F$ (mg/g)(L/mg)$^{1/n}$ is the Freundlich constant, and $n$ is the adsorption intensity.

The experiment was conducted at the optimal conditions with different initial concentrations of 25, 50, 100, 150, 200, 400, 600, and 800 mg/L. The parameters of Langmuir and Freundlich model equations were calculated from the slope and the intercept of the $C_e$ vs. $q_e$/C$_e$ and ln$C_e$ vs. ln$q_e$ plots, respectively, using Origin software. Table 6 illustrates the calculated parameters and regression coefficient $R^2$ of Langmuir and Freundlich isotherm.

As shown in Table 6, that according to the value of $R^2$, the cadmium ions adsorption behavior was more accurately predicted by the Freundlich isotherm model than the Langmuir model indicating the multilayer adsorption with $n$ value greater than 0.5.

In the Langmuir isotherm model, the maximum adsorption capacity ($q_m$) can be regarded as the equilibrium electrosorption capacity [47]. Therefore, the equilibrium electrosorption capacity of the cadmium ions was 3,014.74 mg/g at the optimum conditions. For these two models, the isotherm graphical representations are displayed in Fig. 8.

### 3.5. Adsorption kinetics

The type of sorption mechanism that occurs was identified by testing the experimental data for the adsorption of cadmium Cd(II) ions onto the MnO$_2$/CF composite electrode with the kinetic models namely pseudo-first-order and pseudo-second-order models. The mathematical expressions of these models [46], as linear form, are given in Eqs. (8) and (9), respectively.

$$\ln\left(q_e - q_t\right) = \ln q_e - K_1 t \quad (8)$$

$$\frac{t}{q_t} = \frac{1}{K_2 q_e^2} + \frac{t}{q_e} \quad (9)$$

where $q_e$ (mg/g) and $q_t$ (mg/g) are the adsorption capacities of the adsorbent at equilibrium and $t$ (min), respectively, $K_1$ is the pseudo-first-order rate constant, and $K_2$ is the pseudo-second-order rate constant.

The parameters of the pseudo-first-order and pseudo-second-order models equations were determined from the slope and intercept of the plot of ln($q_e - q_t$) vs. $t$ and $t/q_e$ vs. $t$, respectively, using Origin software Table 7 summarizes the kinetics parameters and the correlation coefficient obtained from these model fits.

It is evident from the results that for cadmium ions removal, the fitting of the experimental data showed a higher correlation coefficient with the best agreement between the calculated and the experimental values of $q_e$ in the pseudo-first-order equation than in the pseudo-second-order equation. Therefore, the electrosorption of Cd(II) ions

Table 6
Determined parameters of Langmuir and Freundlich isotherm models for cadmium

| Isotherm | Parameter | Value |
|---|---|---|
| Langmuir | $q_m$ (mg/g) | 3,014.74 |
| | $b$ | 1.44 × 10$^{-4}$ |
| | $R^2$ | 0.71612 |
| Freundlich | $K_F$ (mg/g)(L/mg)$^{1/n}$ | 0.47591 |
| | $n$ | 1.0257 |
| | $R^2$ | 0.99909 |

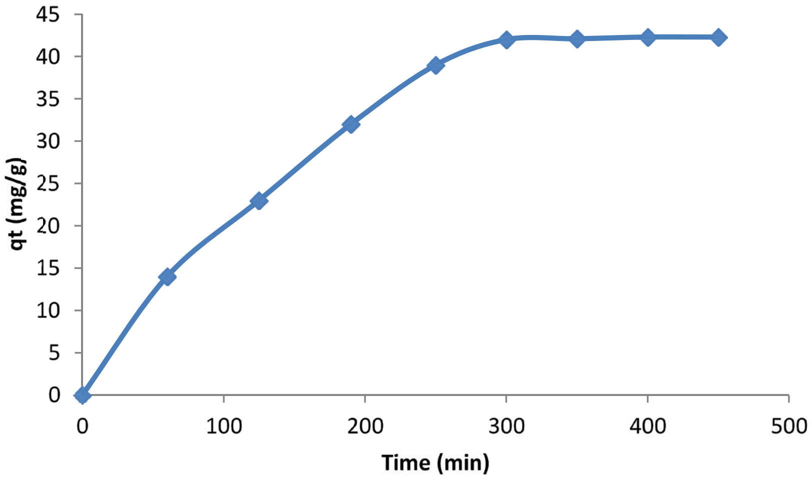

Fig. 7. The adsorption capacity vs. contact time between the MnO$_2$/carbon fiber electrode and the solution at conditions of pH 5.5, 2.6 V, and 2 g/L NaCl concentration for Cd(II) ions removal.

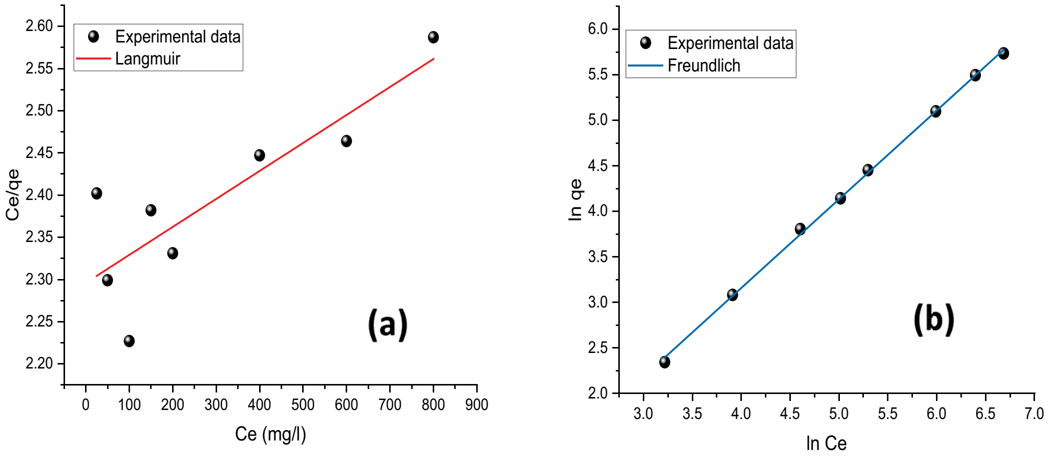

Fig. 8. Adsorption isotherms of cadmium ions on $MnO_2$/carbon fiber at the optimal conditions of 6.03 pH, 2.77 V, and 2.83 g/L NaCl concentration, the data is fitted with: (a) Langmuir model and (b) Freundlich model.

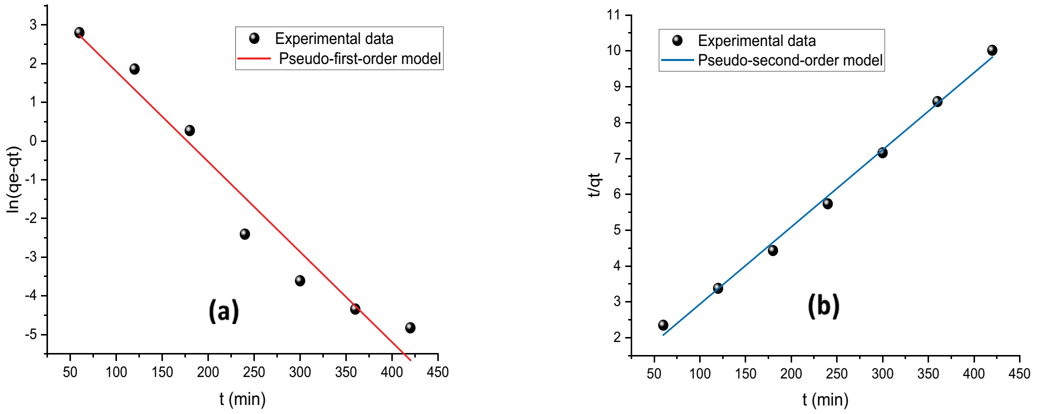

Fig. 9. Kinetic graph for cadmium ions removal onto $MnO_2$/carbon fiber at the optimal conditions of 6.03 pH, 2.77 V, and 2.83 g/L NaCl concentration with Cd(II) initial concentration of 100 ppm, the data is fitted with: (a) pseudo-first-order model and (b) pseudo-second-order model.

Table 7
Determined parameters of pseudo-first-order and pseudo-second-order kinetic models for cadmium ions

| Kinetics | Parameter | Value |
|---|---|---|
| Pseudo-first-order model | $q_e$ (mg/g) | 62.124 |
| | $K_1$ ($min^{-1}$) | 0.023 |
| | $R^2$ | 0.95561 |
| Pseudo-second-order model | $q_e$ (mg/g) | 48.485 |
| | $K_2$ (g/mg)($min^{-1}$) | $5.88 \times 10^{-4}$ |
| | $R^2$ | 0.99529 |

onto $MnO_2$/carbon fiber can be explained accurately by the pseudo-second-order kinetic model. Fig. 9 displays the kinetic graphical representations for the model.

## 4. Conclusions

A $MnO_2$/carbon fibers composite electrode has been successfully synthesized using the anodic electrodeposition process and tested as an electrosorptive electrode for removing cadmium ions from an aqueous solution. The XRD and FESEM results confirm the presence of the $MnO_2$ particles deposited onto the carbon fiber surface with a flower-like nanostructure consisting of many nanorods and with crystalline phase corresponded to $\gamma$-$MnO_2$. The average diameters of the electrodeposited $MnO_2$ nanoparticles were 73.38 nm. The Box–Behnken design of RSM has proven to be a very useful and accurate methodology for optimizing the electrosorption of cadmium ions. The experimental data showed a good fit to the second-order polynomial model with $R^2$ of 0.9817. The cell voltage has the main effect on the cadmium ions removal efficiency with contribution percentage of 60.28%. The optimum conditions were 6.03 pH, 2.77 V, and 3 g/L NaCl concentration resulted in 99.542% removal efficiency. The isotherm study performs that the experimental results of the cadmium ions removal fit very well with the Freundlich model ($R^2$ = 0.99909) with a $q_{max}$ of 3,014.74 mg/g at the optimum conditions, indicating the high adsorption capacity of the prepared electrode. The electrosorption of cadmium ions onto $MnO_2$/CF correlated well with the pseudo-second-order kinetic model.

## Symbols

### Greek

$\alpha$ — Phase of $MnO_2$
$\beta$ — Phase of $MnO_2$
$\gamma$ — Phase of $MnO_2$
$\delta$ — Phase of $MnO_2$
$\theta$ — Angle
$\lambda$ — Wavelength

### Subscripts and superscripts

$q_e$ — Equilibrium adsorption capacity, mg/g
Re — Removal efficiency, %
$C_e$ — Equilibrium concentration, mg/L
$C_0$ — Initial concentration, mg/L
$V$ — Volume of solution, L
$m$ — Total mass of the electrode, mg
$Y$ — Removal efficiency, %
$X_1$ — pH value
$X_2$ — Cell voltage value, V
$X_3$ — Concentration of NaCl, g/L
$x_i$ — Input parameter
$x_j$ — Input parameter
$x_k$ — Input parameter
$a_0$ — Intercept term
$a_i$ — Linear effect
$a_{ii}$ — Squared effect
$a_{ij}$ — Interaction effect
$x_i$ — Coded value of a parameter
$X_i$ — Real value of a parameter
$X_0$ — Real value of a parameter at the center point
$\Delta X_i$ — Step change value
$R^2$ — Multiple correlation coefficient
$q_m$ — Maximum adsorption capacity of the adsorbent, mg/g
$b$ — Langmuir constant of equilibrium adsorption
$K_F$ — Freundlich constant, $(mg/g)(L/mg)^{1/n}$
$n$ — Adsorption intensity
$q_t$ — Adsorption capacity of the adsorbent at t(min), mg/g
$K_1$ — Pseudo-first-order rate constant, $min^{-1}$
$K_2$ — Pseudo-second-order rate constant, (g/mg), $min^{-1}$

### Abbreviations

CDI — Capacitive deionization
EDL — Electrical double layer
TMOs — Transition metal oxides
DC — Direct current
CF — Carbon fiber
XRD — X-ray diffraction
FESEM — Field-emission scanning electron microscopy
EDX — Energy-dispersive X-ray spectrometry
AAS — Atomic absorption spectrometry
MLS — Method of least squares
ANOVA — Analysis of variance
DOF — Degree of freedom
SS — Sum of square
MS — Mean of square
$D_F$ — Desirability function technique
AC — Adsorption capacity
RSM — Response surface methodology
BBD — Box–Behnken design

## References

[1] S. Ayub, A.A. Siddique, Md. S. Khursheed, A. Zarei, I. Alam, E. Asgari, F. Changani, Removal of heavy metals (Cr, Cu, and Zn) from electroplating wastewater by electrocoagulation and adsorption processes, Desal. Water Treat., 179 (2020) 263–271.

[2] A. Azimi, A. Azari, M. Rezakazemi, M. Ansarpour, Removal of heavy metals from industrial wastewaters: a review, ChemBioEng Rev., 4 (2017) 37–59.

[3] F. Fu, Q. Wang, Removal of heavy metal ions from wastewaters: a review, J. Environ. Manage., 92 (2011) 407–418.

[4] C.P.J. Isaac, A. Sivakumar, Removal of lead and cadmium ions from water using *Annona squamosa* shell: kinetic and equilibrium studies, Desal. Water Treat., 51 (2013) 7700–7709.

[5] P. Xu, B. Elson, J.E. Drewes, Chapter 12 – Electrosorption of Heavy Metals with Capacitive Deionization: Water Reuse, Desalination and Resources Recovery, J. Kucera, Ed., Desalination: Water from Water, Scrivener Publishing LLC, United States, 2014, pp. 521–548.

[6] V. Masindi, K.L. Muedi, Chapter 7 – Environmental Contamination by Heavy Metals, H. El-Din M. Saleh, R.F. Aglan, Eds., Heavy Metals, IntechOpen, 2018, pp. 115–133.

[7] P. Chowdhury, A. Elkamel, A.K. Ray, Chapter 2 – Photocatalytic Processes for the Removal of Toxic Metal Ions, S. Sharma, Ed., Heavy Metals in Water: Presence, Removal and Safety, Royal Society of Chemistry, UK, 2014, pp. 25–43.

[8] A. Ahmadi, S. Heidarzadeh, A.R. Mokhtari, E. Darezereshki, H.A. Harouni, Optimization of heavy metal removal from aqueous solutions by maghemite ($\gamma$-$Fe_2O_3$) nanoparticles using response surface methodology, J. Geochem. Explor., 147 (2014) 151–158.

[9] Y. Chen, L. Peng, Q. Zeng, Y. Yang, M. Lei, H. Song, L. Chai, J. Gu, Removal of trace Cd(II) from water with the manganese oxides/ACF composite electrode, Clean Technol. Environ. Policy, 17 (2015) 49–57.

[10] A.H. Abbar, R.H. Salman, A.S. Abbas, Cadmium removal using a spiral-wound woven wire meshes packed bed rotating cylinder electrode, Environ. Technol. Innovation, 13 (2019) 233–243.

[11] Y. Wei, L. Xu, K. Yang, Z. Wang, Y. Kong, H. Xue, Electrosorption of toxic heavy metal ions by mono S- or N-doped and S, N-codoped 3D graphene aerogels, J. Electrochem. Soc., 164 (2017) E17–E22.

[12] E. García-Quismondo, R. Gómez, F. Vaquero, A.L. Cudero, J. Palma, M. Anderson, New testing procedures of a capacitive deionization reactor, Phys. Chem. Chem. Phys., 15 (2013) 7648–7656.

[13] M. Dai, L. Xia, S. Song, C. Peng, J.R. Rangel-Mendez, R. Cruz-Gaona, Electrosorption of As(III) in aqueous solutions with activated carbon as the electrode, Appl. Surf. Sci., 434 (2018) 816–821.

[14] G. Zhou, W. Li, Z. Wang, X. Wang, S. Li, D. Zhang, Electrosorption for organic pollutants removal and desalination by graphite and activated carbon fiber composite electrodes, Int. J. Environ. Sci. Technol., 12 (2015) 3735–3744.

[15] X. Su, T. Alan Hatton, Electrosorption, Kirk-Othmer Encyclopedia of Chemical Technology, John Wiley & Sons, Inc., United States, 2016, pp. 1–11.

[16] C.-H. Hou, C. Liang, S. Yiacoumi, S. Dai, C. Tsouris, Electrosorption capacitance of nanostructured carbon-based materials, J. Colloid Interface Sci., 302 (2006) 54–61.

[17] C.-H. Hou, C.-Y. Huang, A comparative study of electrosorption selectivity of ions by activated carbon electrodes in capacitive deionization, Desalination, 314 (2013) 124–129.

[18] X. Zhao, B. Jia, Q. Sun, G. Jiao, L. Liu, D. She, Removal of $Cr^{6+}$ ions from water by electrosorption on modified activated carbon fibre felt, R. Soc. Open Sci., 5 (2018) 1–13.

[19] C. Hu, F. Liu, H. Lan, H. Liu, J. Qu, Preparation of a manganese dioxide/carbon fiber electrode for electrosorptive removal of copper ions from water, J. Colloid Interface Sci., 446 (2015) 380–386.

[20] X.Z. Wang, M.G. Li, Y.W. Chen, R.M. Cheng, S.M. Huang, L.K. Pan, Z. Sun, Electrosorption of NaCl solutions with carbon nanotubes and nanofibers composite film electrodes, Electrochem. Solid-State Lett., 9 (2006) 23–26.

[21] J.C. Farmer, S.M. Bahowick, J.E. Harrar, D.V. Fix, R.E. Martinelli, A.K. Vu, K.L. Carroll, Electrosorption of chromium ions on carbon aerogel electrodes as a means of remediating ground water, Energy Fuels, 11 (1997) 337–347.

[22] B. Pierozynski, D. Zielinska, Electrosorption of quercetin on glassy carbon electrode, J. Electroanal. Chem., 651 (2011) 100–103.

[23] S.H. Kazemi, M.G. Maghami, M.A. Kiani, Electrodeposited manganese dioxide nanostructures on electro-etched carbon fibers: high performance materials for supercapacitor applications, Mater. Res. Bull., 60 (2014) 137–142.

[24] X. Ma, Y.A. Chen, K. Zhou, P.C. Wu, C.H. Hou, Enhanced desalination performance via mixed capacitive-Faradaic ion storage using $RuO_2$-activated carbon composite electrodes, Electrochim. Acta, 295 (2019) 769–777.

[25] Z. Ye, T. Li, G. Ma, X. Peng, J. Zhao, Morphology controlled $MnO_2$ electrodeposited on carbon fiber paper for highperformance supercapacitors, J. Power Sources, 351 (2017) 51–57.

[26] G. Yu, L. Hu, M. Vosgueritchian, H. Wang, X. Xie, J.R. McDonough, X. Cui, Y. Cui, Z. Bao, Solution-processed graphene/$MnO_2$ nanostructured textiles for high-performance electrochemical capacitors, Nano Lett., 11 (2011) 2905–2911.

[27] R.H. Salman, M.H. Hafiz, A.S. Abbas, Preparation and characterization of graphite substrate manganese dioxide electrode for indirect electrochemical removal of phenol, Russ. J. Electrochem., 55 (2019) 407–418.

[28] M. Amini, H. Younesi, N. Bahramifar, A.A. Lorestani, F. Ghorbani, A. Daneshi, M. Sharifzadeh, Application of response surface methodology for optimization of lead biosorption in an aqueous solution by *Aspergillus niger*, J. Hazard. Mater., 154 (2008) 694–702.

[29] U.K. Garg, M.P. Kaur, D. Sud, V.K. Garg, Removal of hexavalent chromium from aqueous solution by adsorption on treated sugarcane bagasse using response surface methodological approach, Desalination, 249 (2009) 475–479.

[30] Y. Zhao, X. Min Hu, B. Hui Jiang, L. Li, Optimization of the operational parameters for desalination with response surface methodology during a capacitive deionization process, Desalination, 336 (2014) 64–71.

[31] B. Kiran, A. Kaushik, C.P. Kaushik, Response surface methodological approach for optimizing removal of Cr(VI) from aqueous solution using immobilized cyanobacterium, Chem. Eng. J., 126 (2007) 147–153.

[32] Y. Zheng, A. Wang, Removal of heavy metals using polyvinyl alcohol semi-IPN poly(acrylic acid)/tourmaline composite optimized with response surface methodology, Chem. Eng. J., 162 (2010) 186–193.

[33] Y.-H. Liu, H.-C. Hsi, K.-C. Li, C.-H. Hou, Electrodeposited manganese dioxide/activated carbon composite as a high-performance electrode material for capacitive deionization, ACS Sustainable Chem. Eng., 4 (2016) 4762–4770.

[34] B. Choi, S. Lee, C. Fushimi, A. Tsutsumi, Fibrous $MnO_2$ electrode electrodeposited on carbon fiber for a fuel cell/battery system, Electrochim. Acta, 56 (2011) 6696–6701.

[35] C. Liu, J. Wang, J. Tian, L. Xiang, Synthesis and surface characterization of $\gamma$-$MnO_2$ nanostructures, J. Nanomater., 2013 (2013) 1–6.

[36] S. Jana, S. Pande, A.K. Sinha, S. Sarkar, M. Pradhan, M. Basu, S. Saha, T. Pal, A green chemistry approach for the synthesis of flower-like Ag-doped $MnO_2$ nanostructures probed by surface-enhanced raman spectroscopy, J. Phys. Chem. C, 113 (2009) 1386–1392.

[37] Q. Cheng, J. Tang, J. Ma, H. Zhang, N. Shinya, L.C. Qin, Graphene and nanostructured $MnO_2$ composite electrodes for supercapacitors, Carbon, 49 (2011) 2917–2925.

[38] H.Z. Chi, S. Yin, D. Cen, K. Chen, Y. Hu, H. Qin, H. Zhu, The capacitive behaviours of $MnO_2$/carbon fiber composite electrode prepared in the presence of sodium tetraborate, J. Alloys Compd., 678 (2016) 42–50.

[39] M. Toupin, T. Brousse, D. Bélanger, Charge storage mechanism of $MnO_2$ electrode used in aqueous electrochemical capacitor, Chem. Mater., 16 (2004) 3184–3190.

[40] P. Tripathi, V. Chandra Srivastava, A. Kumar, Optimization of an azo dye batch adsorption parameters using Box–Behnken design, Desalination, 249 (2009) 1273–1279.

[41] A. Zirehpour, A. Rahimpour, M. Jahanshahi, M. Peyravi, Mixed matrix membrane application for olive oil wastewater treatment: process optimization based on Taguchi design method, J. Environ. Manage., 132 (2014) 113–120.

[42] B. Ayoubi-Feiz, S. Aber, A. Khataee, E. Alipour, Electrosorption and photocatalytic one-stage combined process using a new type of nanosized $TiO_2$/activated charcoal plate electrode, Environ. Sci. Pollut. Res., 21 (2014) 8555–8564.

[43] D. Ba, I.H. Boyaci, Modeling and optimization: usability of response surface methodology, J. Food Eng., 78 (2007) 836–845.

[44] E. Hazir, T. Ozcan, Response surface methodology integrated with desirability function and genetic algorithm approach for the optimization of CNC machining parameters, Arabian J. Sci. Eng., 44 (2019) 2795–2809.

[45] P.S. Kumar, C. Vincent, K. Kirthika, K.S. Kumar, Kinetics and equilibrium studies of $Pb^{2+}$ ion removal from aqueous solutions by use of nano-silversol-coated activated carbon, Braz. J. Chem. Eng., 27 (2010) 339–346.

[46] N. Lv, X. Wang, S. Peng, H. Zhang, L. Luo, Study of the kinetics and equilibrium of the adsorption of oils onto hydrophobic jute fiber modified via the sol-gel method, Int. J. Environ. Res. Public Health, 15 (2018) 1–14.

[47] X. Zhong, W. Liang, H. Wang, C. Xue, B. Hu, Aluminum-based metal-organic frameworks (CAU-1) highly efficient $UO_2^{2+}$ and $TcO_4^-$ ions immobilization from aqueous solution, J. Hazard. Mater., 407 (2021) 124729, doi: 10.1016/j.jhazmat.2020.124729.